Nat. Volatiles & Essent. Oils, 2021; 8(6): 3369-3383

Synthesis and Characterization of Silver Nanoparticle from *Cyphostemma auriculatum* Roxb.: Its application as antibacterial activity and mode of action

Kishore Mendam[1], S.Jithender Kumar Naik[2*], Anusha C Pawar[3], S.Vamshi[4], V.Mangesh[5], P.Sonu[6]

[1,2,3,4,5,6] Department of Zoology, Osmania University, Hyderabad,India-500007.

Abstract

This investigation demonstrated the accurate reduction and stability of silver nanoparticles (AgNPs) using ethanolic dried *Cyphostemma auriculatum* Roxb. leaf extract as an effective reducing and stabilizing agent. The presence of AgNPs in the colloidal solution was confirmed by the highest absorption peak at 409nm in UV-Vis spectroscopy. According to FTIR significant vibrational spectra obtained from the leaf extract, *Cyphostemma auriculatum* Roxb.leaf extract proteins were primarily responsible for the reduction and stabilization of AgNPs. X-ray diffraction studies were employed to determine the crystal structure of metallic AgNPs. The average particle diameter was calculated using the Debye-Scherrer equation. The SEM images show AgNPs with a rough surface topology and nanoscale dimensions. The researchers created spherical, polydistributed, and monoclinic silver nanoparticles using *Cyphostemma auriculatum* Roxb.(CA-AgNPs) with an average diameter of 15 nm. *Staphylococcus aureus* MTCC 96*, Micrococcus luteus* MTCC 2470*, Klebsiella planticola* MTCC 530, and *Escherichia coli* MTCC 739 had minimum inhibitory concentrations (MICs) of 0.9, 3.9, 1.9, and 1.9 µg/mL, respectively. For the same bacteria, the minimum bactericidal concentration (MBC) values are 1.9, 7.8, 3.9, and 3.9 µg/mL, respectively. The biofilm-inhibiting activity of the CA-AgNPs found to have antibacterial activity in this study was evaluated. *Micrococcus luteus* MTCC 2470 was the most effective at biofilm suppression, with an IC_{50} value of 29.84 g/mL. According to the findings of the cytoplasmic leakage investigation, CA-AgNPs may have caused bacterial strains to rupture their membranes. When the cytoplasmic membrane's permeability is compromised, internal components, primarily potassium ions, leak out. Antibacterial experiments involving ROS formation revealed that oxidative stress in bacterial cells was effective at achieving antibacterial effects. In this study, silver nanoparticles (CA-AgNPs) derived from *Cyphostemma auriculatum* Roxb. green could be used as medicinal agents.

Keywords:*Cyphostemma auriculatum* Roxb., Silver nanoparticle, Antibacterial activity

Introduction

Numerous materials can be used to make nanoparticles. As a result of the wide range of applications, the amount of nanotechnology research being done daily is increasing. The vast majority of scientists and engineers around the world are researching nanoscience and nanotechnology to find new and better applications for them in society and industry. Nanoparticles large surface-area-to-volume ratio and quantum phenomena make them ideal for enhanced data transfer applications. If these properties are altered, they can lead to more advanced applications in a variety of industries, including medicine. Metallic nanoparticles have a large surface area, a confined space, a low defect count, and exceptional chemical, optical, physical, and thermal

properties. Changing the size and shape of a material significantly alters its physical properties, which are very different from those of the corresponding bulk material[1].

For thousands of years, various medicinal plant components have been used in traditional treatments for a wide range of human ailments in many countries around the world. The majority of the world's rural population relies on medicinal herbs that are readily available in their surroundings. *Acalypha indica* (Ahmed et al. 2016)[2], the flowering plant *Dioscorea bulbifera* (Ghosh et al.2015)[3], *Barleria prionitis* (Sougata et al. 2016)[4] ,*Caesalpinia bonducella* (Sukumar and Rudrasenanet al. 2020) [5], *Hagenia abyssinica* (Murthy et al. 2020)[6] and *Mentha longifolia* (Javed et al. 2020) [7] are examples of medicinal plants that have previously been described and used in the green synthesis of AgNPs. In the past, a variety of physical and chemical techniques were used to synthesize AgNPs, necessitating the use of massive amounts of energy as well as other hazardous compounds, resulting in environmental toxicity[8, 9].

Green silver nanoparticles have been used in a variety of applications since the 1970s and 1980s, including photocatalysis, electrocatalysis, and industrial dye degradation [10]. These AgNPs have been shown to inhibit a wide range of microorganisms and bacterial strains. They have distinct properties due to their distinct size, shape, and crystal structure [12]. AgNPs antibacterial, antifungal, antioxidant, anti-angiogenic, and antiplatelet properties previously have been studied in the medical field [13-19]. AgNPs have also been studied for their thrombolytic, anti-diabetic, and anti-cancer properties. *Cyphostemma auriculatum* Roxb.plant can be found in abundance in India, Bangladesh, and Myanmar. Clinging to the wall was a woody plant with cylindrical stems. The leaflets of this plant species are elliptical to ovate, with serrated margins and an acute apex, depending on the species. The design of the leaflet included five to seven smaller veins. Lalitha et al. 2021 [20] investigated the anticancer properties of *Cyphostemma auriculatum* Roxb.using an ethanolic extract of the plant. Historically, indigenous peoples used this plant to treat a variety of diseases, including snake bites and burns. This plant is used as a medicinal herb and blood purifier in cardiac disorders, intestinal worm infections, dog bites, arthritis, purulent wounds, wound healing, tumors, cough and colds, and as a tonic [21–23]. It is also used as a treatment for rheumatoid arthritis. This herb has also been used to treat cases of bloody dysentery and diarrhea in animals [23-28].

The goal of this research is to use *Cyphostemma auriculatum* Roxb.plant leaf extract as an environmentally friendly method of producing AgNPs. As a precursor, silver nitrate is used. In addition to SEM and transmission electron microscopy (TEM), Fourier transform infrared spectroscopy (FTIR) was used to examine the produced CA-AgNPs. Green-synthesized CA-AgNPs were tested for their ability to limit bacterial growth, inhibit biofilm formation, and generate reactive oxygen species (ROS).

Material and Methods

Chemicals

Cyphostemma auriculatum Roxb. is a plant species in the Vitaceae family (grape). The Botanical Survey of India has a Plant Ref. No. BSI/DRC/2019-20/Tech/267 in its database. The silver nitrate precursor for this study was provided by SDFine Chemicals (Mumbai, India). The antibacterial chemicals used in this study were provided by Himedia Laboratories (Mumbai, India). Sigma-Aldrich Chemicals supplied DMSO, fetal bovine serum (FBS), DMEM, penicillin G, and streptomycin for the experiment (St. Louis, USA). The experiment was carried out entirely with double-distilled water.

Preparation of Plant extract

The *Cyphostemma auriculatum* Roxb.plant leaves, handpicked from Mohammadbad village, Mahabubnagar district, Telangana, India, are depicted in Fig.1. Taxonomists from the Botanical Survey of India, Hyderabad, assisted in identifying the plant to preserve the specimens in herbarium form. The leaves were cleaned of dirt by gently washing them with regular water and then with distilled water, as described above. The leaves were dried for fifteen days in the shade at room temperature before being milled into a flour-like product, yielding 1500 g of leaves. In a Soxhlet extractor, 125 grams of leaf powder (125 grams per 1000 milliliters of ethanol) were used for 10 hours until the extractor siphon became colorless. The plant extract was collected using Whatman No. 1 filter paper after it had been filtered through it. The plant extract had to be kept in the refrigerator at 4 ^{o}C until it could be used in the synthesis of AgNPs.

Fig. 1 *Cyphostemma auriculatum* Roxb.plant leaves used in the green synthesis

Synthesis of Silver nanoparticles

AgNPs were synthesized in a single step, following the work of Raju et al. 2020 [26]. An equivalent volume of plant extract(50 mL) was dissolved in 200 mL of freshly prepared silver nitrate (1mM) aqueous solution using a magnetic stirrer at 500 rpm and 40 degrees Celsius. UV-visible

spectroscopy was used to monitor the growth of colloidal silver nanoparticles in a reaction mixture. When the reaction was finished, the color of the reaction mixture changed from pale yellow to dark brown. This was caused by colloidal silver nanoparticles formed in the reaction mixture. The silver nanoparticles were collected after ten minutes of centrifugation at 10000 rpm. The concentrated colloidal silver nanoparticle solution was centrifuged a second time to remove any remaining plant components or phytoconstituents. After rinsing the concentrated colloidal mixture, it was dried in an oven set to 40 degrees Celsius. The silver nanoparticles were scraped and ground into a fine nanopowder, which was then used in higher biological efficiency applications and further research.

Characterization Techniques

The KBr pellet technique was used for FTIR analysis. A pinch of nanopowder was crushed with potassium bromide. The FTIR vibrational spectral data was collected using an IR Affinity-1 type spectrometer from Shimadzu, Japan. FTIR spectra can be investigated directly by placing a small amount of plant leaf extract on the scanning surface. The biosynthesized nanopowder was prepared by dispersing it on a clean slide, and data were collected using a Philips Xpert PRO Instrument with a Cuk X-ray source,with generator settings of 40kV, 30mA, and a scanning rate of 2^{o} min^{-1} in the ϑ=2ϑ configuration. The Debye-Scherrer equation was used to calculate the average grain size of biosynthesized AgNPs.

$$D = \frac{K\lambda}{\beta_{0.5}\ cos\,\theta} \text{ Where } \beta = \frac{\pi}{180\times \mathrm{FWHM}} \quad (1)$$

FWHM is the full width at half maximum (FWHM) of a crystallite, and *D is* the crystallite size, K is the Scherrer constant, which ranges from 0.91 to 1.01 (shape factor), λ is the X-ray wavelength(1.5418 Aº) and ϑ is the Bragg angle.

Following a 30-minute sonication period, the researchers received photos of CA-AgNPs nanopowder suspended in water. A hairdryer was used to dry a drop of the material on a carbon-coated copper grid before the analysis could commence. It was taken with a ZEISS Special Edition 18 SEM, a German-made camera. A water bath with an ultrasonic water bath was used to soak CA-AgNPs nanoparticles for 30 minutes, as previously described. Carbon-coated copper grids were covered with colloidal nanoparticles, and surplus water was filtered away with filter paper before drying for 5-10 minutes. An American-made FEI Tecnai G2S Twin TEM was used to examine the lattice at various magnifications.

Antibacterial efficiency

The well diffusion method was adopted to carry out the antibacterial studies on *Cyphostemma auriculatum* Roxb. green-synthesized silver nanoparticles (CA-AgNPs) in contrast to gram-positive and gram-negative bacterial cultures. The pathogenic reference strains (1.5×10^{8}CFU mL^{-1} equal to 0.5 McFarald standards) and Mueller Hinton broth (MHB) plates were incubated at 30 degrees

Celsius for 24 hours. The samples were dissolved in DMSO at dose ranges between 0.9-500 µg/mL^{-1}. Ciprofloxacin was used as a control. The test bacterial strains used were *Staphylococcus aureus* MTCC 96, *Micrococcus luteus* MTCC 2470, *Klebsiella planticola* MTCC 530, and *Escherichia coli* MTCC 739.

Cytoplasmic leakage

According to [27], cytoplasmic leakage was studied in the treated bacteria by an established technique. After 24 hours of growth at 37 degrees Celsius, the bacteria were transferred to 100 mL of sterile LB medium. To eliminate any leftover cell debris, cultures were centrifuged at 10,000 rpm for 10 minutes and resuspended in sterile NaCl solution (0.85 g/100mL). When the suspension concentrations reached roughly 10^{10} CFU mL^{-1}, they were then fine-tuned. *Staphylococcus aureus* MTCC 96 and *Escherichia coli* MTCC 739 bacterial suspensions (4 mL) were mixed with CA-AgNPs at the MIC values for this experiment. Finally, the suspensions were centrifuged for 10 minutes at 10,000 rpm and the bacterial pellets were removed after an hour of culture at 37°C. At 260 nm and 280 nm, the absorbance of each supernatant was measured (Agilent Cary 60 UV-VIS Spectrophotometer, Agilent Technologies, California, USA). After 30 minutes in a boiling water bath, all bacteria that had developed in the culture sample were killed by a positive control. The negative control was a sample grown without the addition of the test ingredient or the application of heat.

Detection of K^+ ion leakage from the cytoplasm

To investigate the combined effect on the bacterial membrane, CA-AgNP streated bacterial cells were subjected to K^+ leakage assays. Bacterial cells were used in the experiment after being cultured and expanded to the exponential phase. After being treated with CA-AgNPs at their minimum inhibitory concentrations, the cells were incubated for an hour at 37 degrees Celsius. Negative and positive controls were cells that had not been exposed to 70 percent ethanol (50 µL/mL^{-1}). The cells were then extracted by spinning them in a centrifuge for ten minutes at 5000 rpm. The potassium content in the collected supernatant was quantified using ICP-OES [29].

Antibiofilm activity

Gram-negative and Gram-positive bacteria was Bacterium strains were grown in MHB media for 12 hours before being combined and placed in 96 well microtitre plates for 24 hours at 37 degrees Celsius in each well. The biofilm was removed after 12 hours of treatment with silver particles (CA-AgNPs). The biofilms were then dyed for 45 minutes with 0.1 percent crystal violet solution to remove any cells that had not yet been attached. Solubilization and elution of the stained biofilms were performed with 95% ethanoland then dried the plates to remove any excess water. The biofilm absorbance values at 540 nm were measured using an Infinite M200 Pro microtiterplate reader (Tecan). The standard deviations for each of the mixed biofilm experiments were calculated using the average results.

Reactive oxygen species (ROS) detection

Oxidative stress is caused by an increase in reactive oxygen species (ROS) in the bacteria's bodies. A fluorescent molecule known as dichlorodihydrofluorescein diacetate (DCFH2-DA) can detect reactive oxygen species (ROS) and easily pass through cell membranes, where it combines with intracellular ROS to form dichlorofluorescein (DCF), another fluorescent molecule. DCF fluorescence was used to count reactive oxygen species [30]. After 12 hours of incubation, bacteria were inoculated separately into the CA-AgNPs treatment medium and rinsed three times with PBS buffer. The mixture was incubated for 30 minutes at 30°C in a volume ratio of 1:2000 with DCFH2-DA and a new nanosilver-free medium. After incubation, the samples were centrifuged and collected, and PBS was used to clean them. ROS production in bacterial cells was measured using an Infinite M200 Pro microtiter plate reader.

Results and Discussion

UV-visible spectroscopy was used to examine the development and constitution of colloidal metal nanoparticles. This technique is frequently used to investigate metal and metal oxide nanoparticles. Figure 2 shows that, regardless of the amount of $AgNO_3$, the greatest absorption peak occurs at approximately 409 nm in both cases. Because of the appearance of the AgNP peak, it was obvious that the solution contained AgNPs. As a result of surface plasmon resonance(SPR), newly synthesized CA-AgNPs frequently exhibit UV-visible peaks in the 390-450 nm range. Surface plasmon resonance (SPR) is a visual phenomenon caused by the simultaneous oscillation of the surface electrons of metallic nanoparticles. Because of its high intensity and distinct peaks, 1 mM $AgNO_3$ was chosen for further investigation and characterization. Fourier transform infrared spectroscopy is used to investigate the vibrational bands produced by nanoparticles when exposed to infrared radiation.These vibrational bands interact with the metallic nanoparticle surfaces, exposing phytochemicals that are important in the reduction and stabilization processes [31, 32]. Figure 3 depicts FTIR spectroscopy of *Cyphostemma auriculatum* Roxb. green-produced AgNPs and a plant extract. As shown in the image, typical bandwidths are 3443 cm^{-1}, 2353 cm^{-1}, 1636 cm^{-1}, and 1045 cm^{-1}. A large peak at 3443 cm^{-1} [33] can be seen in the spectrum due to stretching vibrations in the –OH group of alcohol or phenolic compounds. Ketones, aldehydes, and carboxylic acids have a wavelength of 2353 cm^{-1} and are assigned to a sharp, high-intensity band at that wavelength. C=O The lower intensity band at 1636cm^{-1}, which is related to molecular stretching vibrations of the C-N and C-C chains, indicates the presence of proteins. The weaker 1045 cm^{-1} band is thought to be caused by protein C-N stretching vibrations. FTIR spectra indicated that *Cyphostemma auriculatum* Roxb. leaf extract proteins were found to play a significant role in reducing and stabilizing AgNPs.

XRD revealed the presence of face-centric cubic crystal structures (111, 200, 220, and 311) in AgNPs, and the peaks were discovered at 2 theta values of 37.81, 45.93, 64.36, and 77.25 are indexed to the

lattice planes of face-centric cubic structures [33]. Scherrer's equation was used to calculate the average particle size, which was 18 nm. A minor peak caused by silver oxide can be found at 31.78 MHz (JCPDS No: 75-1532). Two additional peaks detected the range of 28.35 and 54.59 MHz may be the result of the crystallization of inorganic compounds extracted from the environment. Researchers can examine the surfaces of nanoparticles using a scanning electron microscope (SEM). Figure 5 depicts various magnifications of green-mediated CA-AgNPs. The images show nanoscale CA-AgNPs with a rough surface form. TEM imaging was used to discover CA-AgNP morphological features such as size, shape, and distribution. Figure 6 depicts nanoscale CA-AgNPs with a diameter of 15 nm on average. When CA-AgNPs were created, they were monoclinic, polydistributed, and spherical. According to the XRD data, the computed average size agreed well with the measured average size of the TEM images.

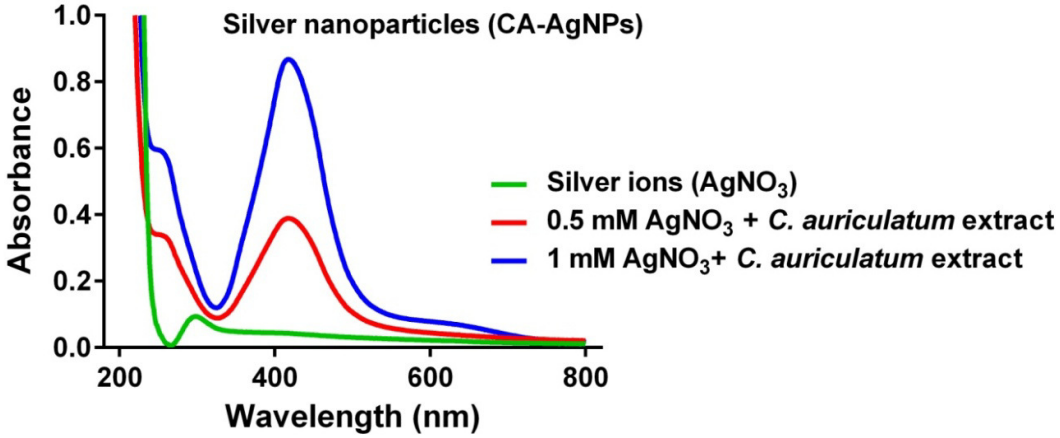

Fig. 2 UV-Vis spectroscopy of green synthesized CA-AgNPs

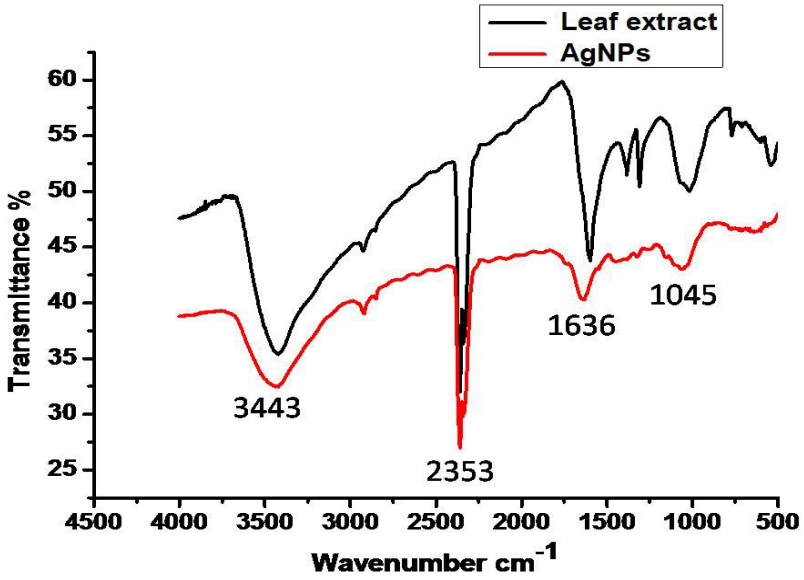

Fig. 3 FTIR spectroscopy of plant extract and green synthesized CA-AgNPs showing vibrational bands

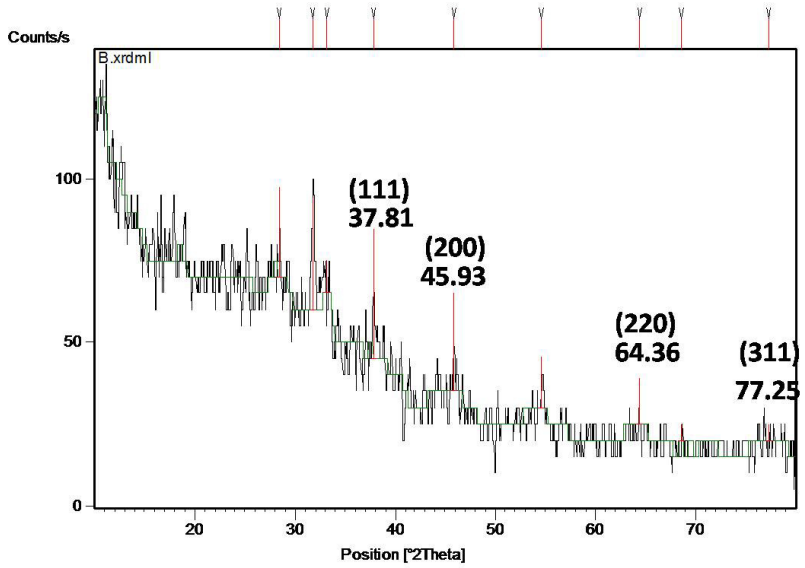

Fig. 4 XRD Spectroscopy of green synthesized CA-AgNPs showings ^{o}2 theta degrees

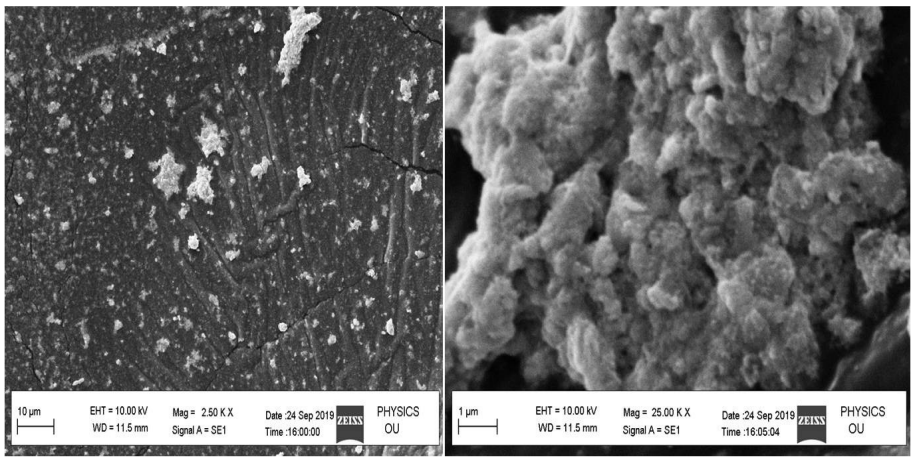

Fig. 5 SEM images of green synthesized CA-AgNPs at various magnifications

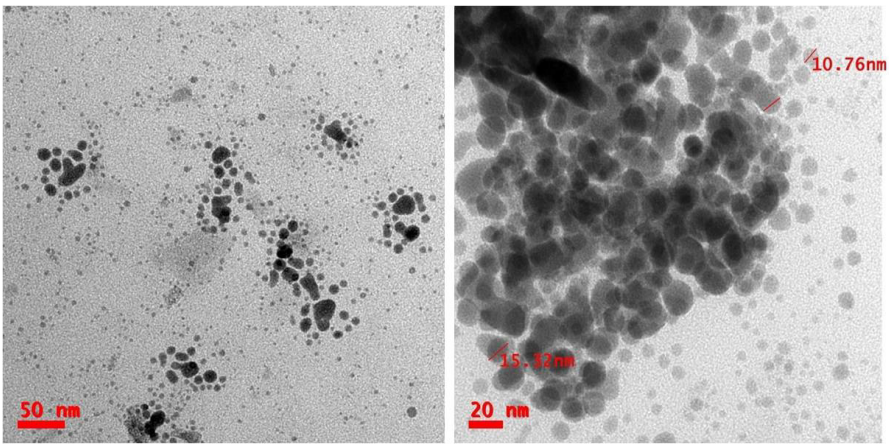

Fig. 6 TEM images of green synthesized CA- AgNPs at various magnifications

Antibacterial activity: MIC and MBC studies

The antibacterial properties of the synthesized CA-AgNPs were investigated using the well- diffusion method. The MIC of each of the three bacteria in the study ranged from 0.9 to 3.9µg/mL, which is consistent with the range of the other bacteria in this study. The minimum inhibitory concentration (MIC) for bacteria *Staphylococcus aureus* MTCC 96, *Escherichia coli* MTCC 739, *Klebsiella planticola* MTCC 530, and *Micrococcus luteus* MTCC 2470 are 0.9, 1.9, 1.9, and 3.9 µg/mL,respectively. The lowest and highest minimum inhibitory concentrations were found in *Staphylococcus aureus* MTCC 96 and *Micrococcus luteus* MTCC 2470, 0.9, and 3.9 respectively. At the minimum bactericidal concentration (MBC) level, the same bacteria had MBC values of 1.9, 3.9, 3.9, and 7.8 µg/mL. *Micrococcus luteus* MTCC 2470 had the highest MBC, while *Staphylococcus aureus* MTCC 96 had the lowest. Ciprofloxacin MIC and MBC values are included as a reference in Table 1.

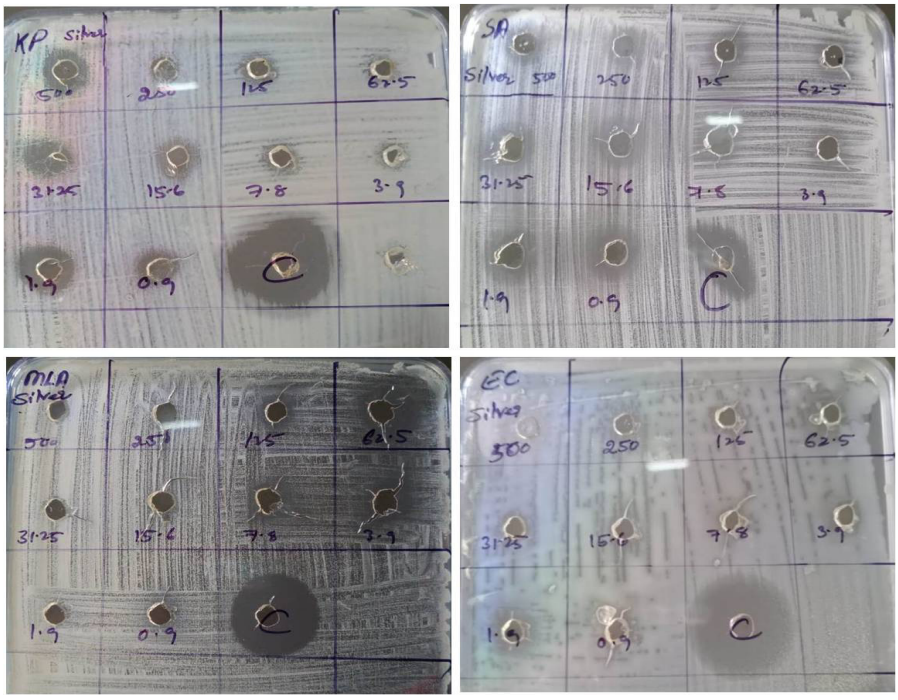

Fig. 7 Antibacterial activity and zone of inhibition against tested bacterial strains

Table 1 Antibacterial activity with MIC and MBC values of CA-AgNPs

Sl. No.	Test strain	Minimum inhibitory concentration (MIC, µg/mL)		Minimum bacterial concentration (MBC, µg/mL)	
		CA-AgNPs	Ciprofloxacin	CA-AgNPs	Ciprofloxacin
1	*E. coli*	1.9	0.9	3.9	1.9
2	*K. planticola*	1.9	0.9	3.9	1.9
3	*S. aureus*	0.9	0.9	1.9	1.9
4	*M. luteus*	3.9	0.9	7.8	1.9

Detection of cytoplasmic leakage from bacterial cell

Researchers were able to determine whether or not nucleotides and proteins were leaking from the bacterial cell suspension by measuring the absorbance of the supernatant collected from the bacterial cell suspension. After 60 minutes of CA-AgNPs exposure, the absorbance at 260 nm of the supernatant of selected *Staphylococcus aureus* MTCC 96, *Micrococcus luteus* MTCC 2470, *Klebsiella planticola* MTCC 530, and *Escherichia coli* MTCC 739 suspensions increased. According to these findings, the contents of the cell are released into the surrounding environment. The absorbance of *Staphylococcus aureus* MTCC 96, *Micrococcus luteus* MTCC 2470, *Klebsiella planticola* MTCC 530, and *Escherichia coli* MTCC 739 suspensions increased at 280 nm after 60 minutes of exposure, indicating the release of cell constituents into the supernatant (Fig. 8b). For both adsorbents tested, *Staphylococcus aureus* MTCC 96 had the highest optical density (OD), while *Micrococcus luteus* MTCC 2470 had the lowest. The results of this experiment were satisfactory when compared to the positive control, indicating that treatment with AgNPs altered membrane permeability, resulting in cytoplasmic membrane leakage.

Detection of K^+ ion leakage from the cytoplasm

The ability of a bacterial cell to maintain membrane potential is critical to its survival. Potassium leakage is common when a cell's membranes are compromised. When cytoplasmic potassium leakage was discovered, it was determined that the bacterial membrane had been ruptured. CA-AgNPs increased the outflow of potassium from the microorganisms *Staphylococcus aureus* MTCC 96 and *Escherichia coli* MTCC 739, *Klebsiella planticola* MTCC 530, and *Micrococcus luteus* MTCC 2470 as shown in Fig. 9. When CA-AgNPs wasadded to the solution, sodium efflux increased as well. According to these findings [35], CA-AgNPs disrupt bacterial membranes, allowing internal components such as potassium ions to escape the cell. At both the highest and lowest concentrations, *Micrococcus luteus* MTCC 2470 was found to least potassium leakage *and Staphylococcusaureus* MTCC 96 had the most potassium leakage. Damage to the cell membrane reduces the potassium gradient across the membrane, affecting membrane function and eventually leading to cell death [36].

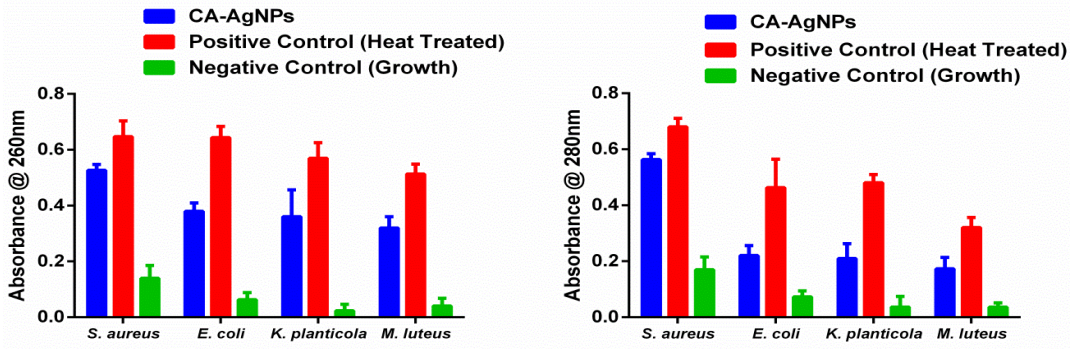

Fig. 8 a) Measurement of cytoplasmic leakageandabsorbance at 260 nm and b) absorbance at 280nm

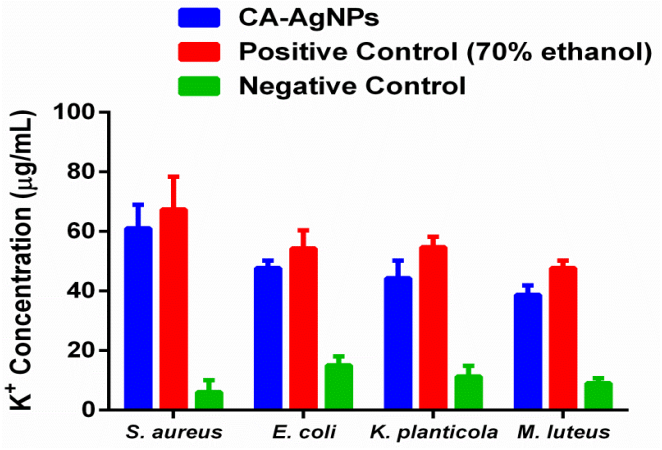

Fig. 9 Measurement of cytoplasmic K^+ ion leakage

Antibiofilm activity

Cells in a biofilm collaborate to form a layer on a living or nonliving surface that is wrapped in a self producedexopolysaccharide and protein-rich polymeric matrix [37, 38]. These biofilms are resistant to antimicrobials, resulting in long-term infections in both hospital and community settings [39]. Researchers looked into the compound's ability to suppress bacterial biofilm formation to learn more about its antibacterial potential. CA-AgNPs were tested for biofilm inhibition activity, and the results revealed that the compounds have antibiofilm activity. The IC_{50} values for CA-AgNPs against all of the bacterial strains tested are shown in Fig. 10. *Micrococcus luteus* MTCC 2470 had the highest biofilm inhibition activity, at 29.84 µg/mL.*Staphylococcus aureus* MTCC 96, on the other hand, had the lowest biofilm inhibition activity, with an IC_{50} value of 10.13 µg/mL.

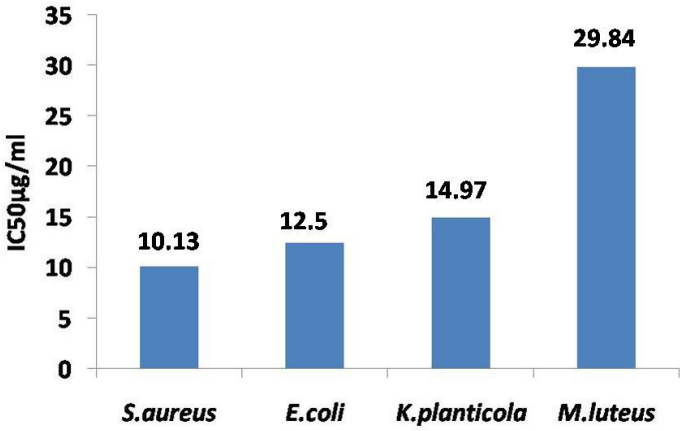

Fig. 10 Antibiofilm activity of green synthesized CA-AgNPs

ROS levels during bactericidal action of CA-AgNPs

The bacteria used in the antibacterial activity and ROS generation experiments were *Staphylococcus aureus* MTCC96, *Micrococcus luteus* MTCC 2470, *Klebsiella planticola* MTCC530, and *Escherichia coli*

MTCC739. Bacterial strains produce reactive oxygen species over time. Figure 11 shows an example of this. According to the data, *Staphylococcus aureus* MTCC 96 had the highest OD (0.68) and *Micrococcus luteus* MTCC 2470 lowest generation OD (0.38). ROS are oxygen-based molecules that are extremely reactive. Hydroxyl radicals ($^{\cdot}OH$), superoxide anions (O_2^-), singlet oxygen ($^1O_2$) and hydrogen peroxide (H_2O_2) are examples of oxidation products. One of the ways CA-AgNPs cause toxicity is through the generation of reactive oxygen species (ROS). In the presence of CA-AgNPs, hydrogen peroxide undergoes radical synthesis, yielding hydroxide ions, and hydroxyl radicals. When CA-AgNP was present, it generated hydroxyl radicals and reactive oxygen species (ROS). These enzymes, such as SOD and glutathione, aid in the protection of cells from oxidative stress. ROS has been shown in studies to be capable of activating SOD and GSH to maintain a balance of oxidative and antioxidant levels. Oxidative stress occurs when antioxidant defense mechanisms are unable to keep up with excessive ROS generation. Reactive oxygen species (ROS) and oxidative stress cause lipid peroxidation. ROS, in addition to causing apoptosis and DNA damage, also inhibits ATP production, ultimately leading to cell death [41, 42].

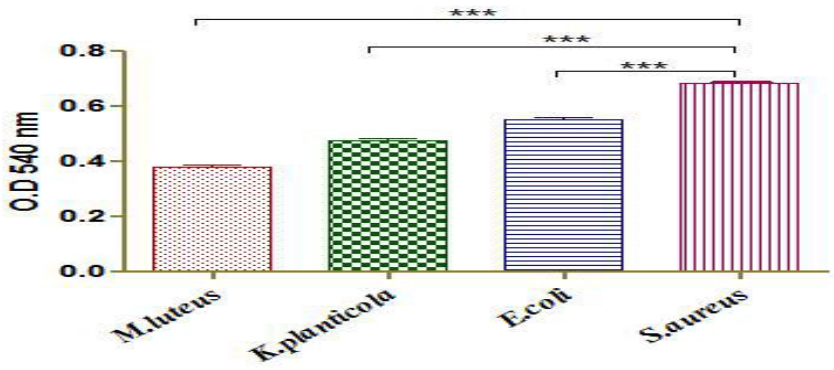

Fig. 11 ROS of various bacteria treated with green synthesized CA-AgNPs

Conclusions

The plant *Cyphostemma auriculatum* Roxb.extract was used as a catalyst in the synthesis of AgNPs. This procedure is both environmentally friendly and cost-effective, and it has no negative effects on the environment. The phytoconstituents from the plant extract passivating agents stabilized the AgNPs by binding to the surface and were successfully detected using Fourier transform infrared spectroscopy through the vibrational bands.Scanning electron microscopy and transmission electron microscopy were used to investigate the morphology of AgNPs mediated by plants. According to the study, the average particle size was 15 nm. The synthesized particles were monoclinic, polydistributed, and slightly aggregated. The antibacterial efficiency of these plant-mediated AgNPs was investigated using standard clinical bacterial strains in terms of MIC and MBC and showed good activity. The treatment of CA-AgNPs disrupted membrane permeability and increased K^+ ion leakage

into the surrounding environment. Antibacterial CA-AgNPs were tested to see if they could inhibit biofilm formation. CA-AgNPs showed modest-to-goodbiofilm inhibition ability against all investigated bacterial strains. Metallic nanoparticles containing physiologically active phytochemicals derived from medicinal plants play an important role in the development of new and efficient industrial and pharmaceutical processes and products.

Acknowledgment: Authors are thankful tothe central facility for research and development,Osmania University,Hyd and central analytical facility,University College of Technology, Osmania University,Hyd and Department of Zoology, Osmania University,Hyd and Department of Physics, Osmania university, Hyd and Department of Biochemistry, Osmania university, Hyd for providing facilities to carry out the research work.

Conflict of Interest: The authors declare that they don't have any conflict of interest.

References

1. Albrecht M. A., Evans C. W., Raston C. L., (2006), Green chemistry and the health implications of nanoparticles. *Green Chem*. 8: 417-432.
2. Ahmed S, Ahmad M, Swami BL, Ikram S (2016) A review on plants extract mediated synthesis of silver nanoparticles for antimicrobial applications: a green expertise. J Adv Res 7:17–28. https ://doi. org/10.1016/j.jare.2015.02.007
3. Ghosh S, Jagtap S, More P et al (2015) *Dioscoreabulbifera*mediated synthesis of novel au core ag shell nanoparticles with potent antibiofilm and antileishmanial activity. J Nanomater 2015:1–12. https ://doi.org/10.1155/2015/562938
4. Sougata G, Maliyackal JC, Ashwini NH et al (2016) Nanomedicine& nanotechnology *barleriaprionitis*leaf mediated synthesis of silver and gold. J NanomedNanotechnol https ://doi.org/10.4172/2157-7439.100039
5. Sukumar S, Rudrasenan A (2020) Green synthesis of Cu/Cu2O/CuO nanostructures and the analysis of their electrochemical properties. ACS Omega 5:1040. https ://doi.org/10.1021/acsom ega.9b028 57
6. Murthy HCA, Desalegn T, Kassa M et al (2020) Synthesis of green copper nanoparticles using medicinal plant *Hageniaabyssinica* (Brace) JF. Gmel. leaf extract: antimicrobial properties. J Nanomater 2020:1–12. https ://doi.org/10.1155/2020/3924081
7. Javed B, Nadhman A, Mashwani Z-R (2020) Phytosynthesis of Ag nanoparticles from Menthalongifolia: their structural evaluation and therapeutic potential against HCT116 colon cancer, Leishmanial and bacterial cells. ApplNanosci. https ://doi.org/10.1007/s1320 4-020-01428 -5
8. Otunola, G.A.; Afolayan, A. In Vitro Antibacterial, Antioxidant and Toxicity Profile of Silver Nanoparticles Green-Synthesized and Characterized from Aqueous Extract of a Spice Blend Formulation. J. Biotechnol. Biotechnol. Equip. 2018, 32, 724–733.
9. Salam, H.A.; Rajiv, P.; Kamaraj, M.; Jagadeeswaran, P.; Gunalan, S.; Sivaraj, R. Int. Res. J. Biol. Sci 2012, 1, 85–90.
10. Ananda Murthy HC, Prakash CH, Abebe B, Shanthaveerayya K (2020) Current research in science and technology, vol 4. Book Publisher International (a part of SCIENCEDOMAIN International), India

11. Hemmati S, Harris MT, Barkey DP (2020) Polyol silver nanowire synthesis and the outlook for a green process. J Nanomater 2020:1– 25. https ://doi.org/10.1155/2020/9341983
12. Parashar V., Parashar R., Sharma B., Pandey A.C. Parthenium leaf extract mediated synthesis of silver nanoparticles of silver nanoparticles: A novel approach towards weed utilization. Dig. Jou. Nanomater. Biostructur, 2009; 4(1): 45-50.
13. Elegbede, J. A.; Lateef, A. Nanotechnology and Nanomaterial Applications in Food, Health, and Biomedical Sciences. Verma, D.K., Goyal, M.R., Suleria, H. A. R., Eds.; Apple Academic Press: Boca Raton, 2019; pp 328.
14. Agbaje, L.; Elegbede, J.A.; Akinola, P.O.; Ajayi, V.A. Biomedical Applications of Green Synthesized-Metallic Nanoparticles: A Review. Pan African J. Life Sci. 2019, 3, 157–182.
15. Badmus, J.A.; Oyemomi, S.A.; Adedosu, O.T.; Yekeen, T.A.; Azeez, M.A.; Adebayo, E.A.; Lateef, A.; Badeggi, U.M.; Botha, S.; Hussein, A.A.; Marnewick, J.L. Heliyon 2020, 6, e05413.
16. Aina, D.A.; Owolo, O.; Lateef, A.; Aina, F.O.; Hakeem, A.S. Karbala Int. J. Mod. Sci. 2019, 5, 71–80.
17. Oladipo, I.C.; Lateef, A.; Azeez, M.A.; Asafa, T.B.; Yekeen, T.A.; Irshad, S.B.; Abbas, H.M.; H, S. IOP Conf. Ser. Mater. Sci. Eng. 2020, 805, 012035.
18. Lateef A.; Ojo S.A.; Elegbede J.A.; Akinola P.O.; Akanni E.O. in Environmental Nanotechnology. Environmental Chemistry for a Sustainable World. Dasgupta, N., Ranjan, S., Lichtfouse, E., eds.; Springer: Cham, 2017; pp 243–277.
19. Gomathi, A.C.; Xavier Rajarathinam, S.R.; Mohammed Sadiq, A.; Rajeshkumar, S. Anticancer Activity of Silver Nanoparticles Synthesized Using Aqueous Fruit Shell Extract of Tamarindusindica on MCF-7 Human Breast Cancer Cell Line. J. Drug Deliv. Sci. Technol. 2020, 55, 101376.
20. S. Lalitha1, D. Anusha2,*, Yogeshkumar Murkunde3, Viji Devanand4, K.Maheshkumar5, Anti-Cancer Activity of *CayratiaAuriculata*Ethanolic Extracts Against Cancer Cell Line A549 - An *In Vitro* Analysis,Pharmacogn J. 2021; 13(2): 495-499.
21. Saheb TS. A Study on Medicinal Climbers of Nallamalais, Andhra Pradesh. *International Journal of MultidisciplinaryResearch and Development* 2014;1:172-176.
22. Srivastava A, Patil SP, Mishra RK, et al. Ethnomedicinal importance of the plants of Amarkantak region, Madhya Pradesh,India. *Int J Med Arom Plants* 2012;2:53-59.
23. Wath M, Sangeeta JS. Ethnoveterinary survey of herbal therapy treating livestocks of Melghat region (Maharashtra). *IJPAES* 2014;3:42-48.
24. Patil US, Deshmukh OS. Traditional ethno-veterinary practices in Betul district Madhya Pradesh India. *International Journal of Current Researchin Life Sciences* 2015; 4:423-428.
25. RajuSandupatla, Ashok Dongamanti, Rama Koyyati, Antimicrobial and antioxidant activities of phytosynthesized Ag, Fe and bimetallic Fe-Ag nanoparticles using Passifloraedulis: A comparative study, Materials Today: Proceedings 44 (2021) 2665–2673
26. S. Raju, D. Ashok, Ch. Vinuthna, Comparative Antimicrobial Activity of Phytofabricated Ag and Au Nanoparticles from L*edebouriahydrabadensis*Rhizome using Various Methods, Indian J Pharm Sci 2020;82(5):851-860

27. ArunaJyothiKora, RaoBeeduSashidhar, Antibacterial activity of biogenic silver nanoparticles synthesized with gum ghatti and gum olibanum: a comparative study, The Journal of Antibiotics (2015), https://doi.org/10.1038/ja.2014.114.
28. L. Rastogi, A.J. Kora, R.B. Sashidhar, Antibacterial effects of gum kondagogu reduced/ stabilized silver nanoparticles in combination with various antibiotics: amechanistic approach, Appl. Nanosci. 5 (2015) 535–543, https://doi.org/10.1007/ s13204-014-0347-9.
29. K. Tiede, A.B.A. Boxall, X. Wang, D. Gore, D. Tiede, M. Baxter, H. David, S.P. Tear, J. Lewis, Application of hydrodynamic chromatography-ICP-MS to investigate the fate of silver nanoparticles in activated sludge, J. Anal. At. Spectrom. 25 (2010) 1149–1154, https://doi.org/10.1039/b926029c.
30. Wahab R, Khan F, Yang Yb, Hwang IH, Shin H-S, Ahmad J, et al. Zinc oxide quantum dots: multifunctional candidates for arresting C2C12 cancer cells and their role towards caspase 3 and 7 genes. RSC Advances. 2016; 6(31):26111–20. https://doi.org/10.1039/c5ra25668b.
31. Makarov, V.V.; Love, A.J.; Sinitsyna, O.V.; Makarova, S.S.; Yaminsky, I.V.; Taliansky, M.E.; Kalinina, N.O. "Green" Nanotechnologies: Synthesis of Metal Nanoparticles Using Plants. ActaNaturae. 2014, 6, 35–44.
32. Ananda Murthy, H.C. Nanochem. Res. 2020, 5 (2), 128–140
33. Salmen, S.H.; Alharbi, S.A. Silver Nanoparticles Synthesized Biogenically from Aloe fleurentiniorum Extract: Characterization and Antibacterial Activity. Green Chem. Lett. Rev 2020, 13, 1–5.
34. Ismail M, Khan MI, Khan SB, Akhtar K, Khan MA, Asiri AM. Catalytic reduction of picric acid, nitrophenols and organic azo dyes via green synthesized plant supported Ag nanoparticles. J Mol Liq. 2018;268:87–101
35. Ismail M, Gul S, Khan MI, Khan MA, Asiri AM, Khan SB. Medicagopolymorpha-mediated antibacterial silver nanoparticles in the reduction of methyl orange. Green Process Synth. 2019;8:118–27.
36. A. Pena, N.S. Sanchez, M. Calahorra, Effects of chitosan on candida albicans: conditions for its antifungal activity, Biomed. Res. Int. 2013 (2013), https://doi.org/ 10.1155/2013/527549.
37. R. M. Donald, *Emerg Infect Dis.* 2002, *8*, 881–890.
38. J. W. Costerton, K. J. Cheng, G. G. Geesey, T. I. Ladd, J. C. Nickel, M.Dasgupta, T, J. Marrie, *Annu Rev Microbiol.* 1987, *41*, 435–464.
39. T. F. Mah, G. A. O'Toole, *Trends Microbiol.* 2001, *9*, 34–39.
40. Hou J, You G, Xu Y, Wang C, Wang P, Miao L, et al. Antioxidant enzyme activities as biomarkers of fluvial biofilm to ZnO NPs ecotoxicity and the Integrated Biomarker Responses (IBR) assessment. Ecotoxicol Environ Saf. 2016; 133:10–7. https://doi.org/10.1016/j.ecoenv.2016.06.014.
41. Gurunathan S, Qasim M, Park C, Yoo H, Kim JH, Hong K. Cytotoxic Potential and Molecular Pathway Analysis of Silver Nanoparticles in Human Colon Cancer Cells HCT116. International journal of molecular sciences. 2018; 19(8). https://doi.org/10.3390/ijms19082269 .
42. Gopinath V, Priyadarshini S, Al-Maleki AR, Alagiri M, Yahya R, Saravanan S, et al. In vitro toxicity, apoptosis and antimicrobial effects of phyto-mediated copper oxide nanoparticles. RSC Advances. 2016; 6(112):110986–95. https://doi.org/10.1039/c6ra13871c.